Int. J. Heat Mass Transfer. Vol. 28, No. 1, pp. 265–276, 1985
Printed in Great Britain

0017–9310/85 $3.00 + 0.00

Effects of shear on the turbulent diffusivity tensor

S. TAVOULARIS
Department of Mechanical Engineering, University of Ottawa, Ottawa, Ontario K1N 6N5, Canada

and

S. CORRSIN
Department of Chemical Engineering, The Johns Hopkins University, Baltimore, MD 21218, U.S.A.

(*Received* 31 *March* 1983 *and in revised form* 7 *June* 1984)

Abstract—Earlier measurements of some components of the turbulent diffusivity tensor D_{ij} in a nearly homogeneous turbulent shear flow with constant mean temperature gradient parallel to the mean shear are now supplemented with measurements of additional components in the same flow but with a mean temperature gradient perpendicular to both mean velocity and mean shear. A quasi-Lagrangian analysis provides expressions for all components of D_{ij} and confirms the expectation that D_{ij} is non-diagonal and non-symmetric. The analysis also suggests the possibility that D_{11} and D_{21} might become positive at sufficiently large values of mean shear. Independent estimates of D_{ij} based on a numerical simulation of homogeneous shear flow as well as on a rapid distortion type analysis are also reported.

1. INTRODUCTION

THE MOST widely used approximations in the modeling of turbulent heat transport are based on the assumption that the turbulent heat flux, $-\overline{\theta u_i}$, $i = 1, 2, 3$ and the mean temperature gradient $\partial\bar{T}/\partial x_i$ are proportional. It has long been known that such a relationship is often wrong in principle, yet can be useful in practice [1]. Even a simple scalar proportionality coefficient ("turbulent diffusivity" or "eddy diffusivity") has sometimes been successful in rough predictions of the mean temperature field in several shear flows, but it has been found inadequate for the general modeling of non-isotropic turbulence [2, 3]. The appropriate form of the diffusivity concept, if it is to be used, is a second-rank "turbulent diffusivity tensor", D_{ij} [4], defined by

$$-\overline{\theta u_i} \equiv D_{ij}\frac{\partial\bar{T}}{\partial x_j}. \tag{1}$$

It has been shown (for a formal proof, see [5]) that D_{ij} cannot be diagonal, except in isotropic turbulence, where it is proportional to the unit tensor. The first theoretical evaluation of the components of D_{ij} is due to Batchelor [4], who generalized Taylor's [6] diffusion theory to express D_{ij} in terms of the Lagrangian velocity correlation in statistically stationary, unsheared, homogeneous, non-isotropic turbulence. However, for most practical situations, the effects of shear must be included. Obviously, the explicit form of D_{ij} depends on the choice of coordinate system, $x_i, i = 1, 2, 3$. In nearly-parallel shear flows, a convenient Cartesian system consists of the local direction, x_1, of the mean speed $\bar{U}_1$, the direction, x_2, of the dominant mean shear, and the normal direction, x_3, often a direction of approximate homogeneity.

The few existing estimates of non-diagonal components of D_{ij} are based on rather intuitive arguments. The pioneering analysis by Eckart [7] has shown that the presence of shear in a laminar flow effectively increases the mean concentration gradients, but Lettau [8] was the first to offer an explicit, semi-empirical expression for a non-diagonal component, D_{12}. Lettau's further assumption that $D_{21} \simeq 0$ was contested by Matsuoka [9], who concluded that $D_{21} \simeq D_{12}$. implying that D_{ij}, although not diagonal, is symmetrical. Gee and Davies [10] then modified Matsuoka's arguments and suggested that $D_{21} \simeq \frac{1}{2}D_{12}$. Yaglom [11] showed qualitatively that both D_{12} and D_{21} are negative in a shear flow with positive shear and negative mean temperature gradient.

In principle, the components of D_{ij} can be measured directly via the definition, equation (1). However, relevant measurements in specially designed experimental configurations are rather scarce. Rough computations of some components from available data have been presented by Yaglom [11] for the atmospheric boundary layer, and by Corrsin [1] for a laboratory boundary layer and an axisymmetric jet. The accuracies were limited by uncertainties in the directions of the mean gradients. In any case, the only components so far determined with some confidence have been D_{22} and D_{12}.

As an especially simple case for detailed measurement of the components of D_{ij}, we consider a transversely homogeneous turbulent shear flow, i.e. a flow with a constant mean velocity gradient $\mathrm{d}\bar{U}_1/\mathrm{d}x_2$ and transversely uniform (though increasing downstream) turbulent stresses $-\overline{u_iu_j}$ and velocity integral scales. This flow retains many of the crucial features of more complex common turbulent shear flows while allowing a relatively simple analytical

NOMENCLATURE

D_{ij}	turbulent diffusivity tensor
h	wind-tunnel height
K_1, K_2	time scale parameters
$L_{11,1}$	Eulerian streamwise velocity integral length scale
M_{ij}	Eulerian velocity correlation moment in a moving frame
M_{ij}	Lagrangian velocity correlation moment
M_{ij}^*	quasi-Lagrangian velocity correlation moment
R_{ij}	Eulerian velocity correlation coefficient
$R_{\lambda 1}$	turbulence Reynolds number
t	time
T	temperature
T_{ij}	Eulerian velocity integral time scale in a moving frame
T_{ij}	Lagrangian velocity integral time scale
T_{ij}^*	quasi-Lagrangian velocity integral time scale
u_i	Eulerian velocity fluctuation
$\bar{U}_1$	mean velocity
$\bar{U}_c$	centreline mean velocity
v_i	Lagrangian velocity fluctuation
v_i^*	quasi-Lagrangian velocity fluctuation
V_i	Lagrangian velocity
x_1	streamwise coordinate, distance from flow origin
x_2	coordinate in the direction of mean shear
x_3	spanwise coordinate.

Greek symbols

γ	molecular diffusivity
δ_{ij}	Kronecker delta
ΔT	temperature rise
η	Kolmogorov microscale
θ	temperature fluctuation in Eulerian coordinates
ϑ	temperature fluctuation in Lagrangian coordinates
λ_{11}	streamwise Taylor microscale
ν	kinematic viscosity
τ	total strain, time increment.

Suffixes

$(\bar{\cdots})$	time-averaged quantity
$(\cdots)'$	root mean squared value
$(\cdots)_c$	value on the wind-tunnel axis
$(\underset{\sim}{\cdot})$	vector quantity.

representation. The present experiments correspond to roughly the same mean shear as the ones reported by Harris *et al.* [12] and by Tavoularis and Corrsin [13], which demonstrated a self-preserving turbulence structure over an extensive part of the test volume.

The direct measurement of all D_{ij} components requires the generation of mean temperature gradients in all three directions, x_i, $i = 1, 2, 3$. It is simplest to study three separate cases, those with temperature gradients which are reasonably uniform and in turn aligned with each of the Cartesian axes (Fig. 1). Of course, the gradient constancy can be only approximate due to practical (wind-tunnel boundary layer growth) as well as conceptual restrictions. The case with mean temperature gradient parallel to mean velocity gradient ($\partial\bar{T}/\partial x_2 \simeq$ constant and $\partial\bar{T}/\partial x_1 = \partial\bar{T}/\partial x_3 \simeq 0$), reported earlier [13], permits the determination of D_{12} and D_{22} ($D_{32} \simeq 0$ by symmetry).

New experiments in the same flow field, but with the mean temperature gradient approximately normal to both mean velocity and to mean velocity gradient ($\partial\bar{T}/\partial x_3 \simeq$ constant and $\partial\bar{T}/\partial x_1 \simeq \partial\bar{T}/\partial x_3 \simeq 0$), described in the next section, allow the determination of D_{i3}, $i = 1, 2, 3$. A third case, that with a dominant streamwise mean temperature gradient ($|\partial\bar{T}/\partial x_1| \gg |\partial\bar{T}/\partial x_2|$, $|\partial\bar{T}/\partial x_3|$), is currently under development.

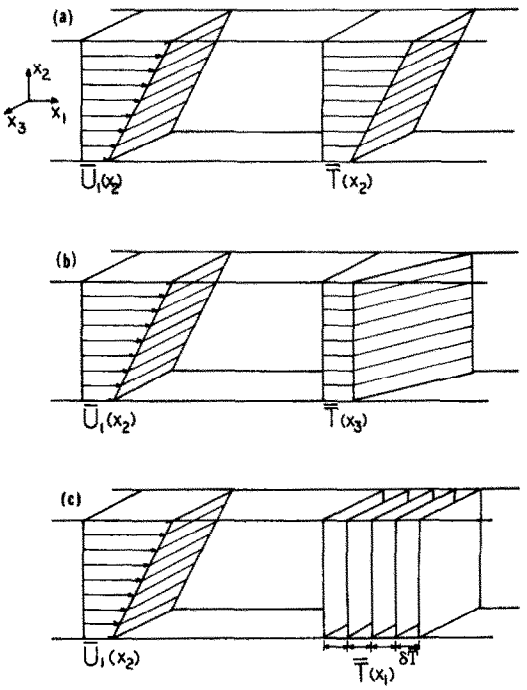

FIG. 1. Sketch showing the orientations of the mean shear and of the mean temperature gradients (a) $d\bar{T}/dx_2 \neq 0$, (b) $d\bar{T}/dx_3 \neq 0$, (c) $d\bar{T}/dx_1 \neq 0$. In all cases $d\bar{U}_1/dx_2 =$ const.

Theoretical estimation of D_{ij} components in exactly or nearly homogeneous turbulent shear flows also is simpler than that in more general flows. Deissler [14] examined analytically the case of weakly sheared, homogeneous, small Reynolds number turbulence with temperature gradient parallel to the mean shear, and Fox [15] extended this study by including a lateral temperature gradient as well. They used a "covariance discard" approximation to close the indeterminate set of moment equations.

A quasi-Lagrangian analysis of fluid point dispersion in (postulated, physically unrealizable) stationary, homogeneous, turbulent shear flow by Corrsin [16, 17], was exploited by Riley and Corrsin [18] to estimate the diagonal components of D_{ij}, and the sum $D_{12}+D_{21}$. A slightly different application of the same viewpoint, allowing estimation of D_{12} and D_{21} individually and, thus, emphasizing the non-symmetry of D_{ij} will be presented in Section 3. A preliminary version of this analysis has been presented by Corrsin [19], while a similar procedure which, however, produces distinct results has been explored by Lumley [20]. The present theoretical expressions are evaluated roughly by using experimental velocity scale results, and the numbers are compared with the direct heat flux measurements. A different test of the theoretical estimates will be made by appeal to a crude numerical simulation of homogeneous turbulent shear flow outlined by Riley and Corrsin [21] (details given in [22]). As an additional example, independent estimates of D_{ij} components will be based on a rapid distortion type analysis by Kozlov and Sabel'nikov [23]. All estimates are presented in Section 4.

The present study is restricted to exactly or approximately homogeneous turbulence, where the concept of a diffusivity tensor is physically sound. More sophisticated closure schemes for scalar transport [3] would be necessary for inhomogeneous or wall-bounded flows. Although techniques such as k–ε modeling have occasionally met with success (e.g. [24] for pipe flow) they necessarily involve arbitrary coefficients, while the present approach is based on primary flow variables only.

2. EXPERIMENTAL RESULTS

The flow field

Experiments were conducted in a nearly homogeneous turbulent shear flow, which was essentially identical with the flows described in [12] and [13]. The flow was generated in an open discharge wind-tunnel with a 30.5 × 30.5 cm square, 330 cm long, test section. The shear flow generator, located at the upstream end of the test section, consisted of a set of ten parallel channels, each 2.54 cm wide, separated by rigid aluminum plates. Screens of various numbers, mesh sizes, and solidities controlled the mean speed individually in each channel, thus generating an array of jets discharging at differing speeds. As shown in the previous two publications, the mean shear $d\bar{U}_1/dx_2$ thus generated remained essentially constant in the test section, while the turbulent velocities and the integral length scales increased monotonically downstream (after an initial adjustment interval) while preserving a reasonable transverse homogeneity away from the walls. The shear stress correlation coefficient was roughly constant, about -0.45. In general, the turbulent field appeared to evolve in a self-similar manner over an appreciable part of the test section, corresponding to non-dimensional "total strains" $\tau = (x_1/\bar{U}_c)\, d\bar{U}_1/dx_2$ in the range 4.5–12.5 ($\bar{U}_c$ is the centreline mean speed).

The downstream developments of the mean squared turbulent velocities and of the shear stress correlation coefficient are shown in Fig. 2. The non-uniformities of the r.m.s. velocity fluctuations in the x_2-direction were less than 15% in the tunnel core. Figure 3 contains profiles of the mean velocity and of the r.m.s. (denoted by primes) velocity fluctuations in the x_3-direction. Although u_1' shows a systematic deviation as high as 20% from its centerline value, all other examined quantities are sufficiently uniform (within $\pm 10\%$) in the central core of the wind-tunnel, occupying nearly half of the cross-section. For convenience in later computations, some relevant velocity field data are summarized as follows ($\tau = 11.0$)

$$\bar{U}_c \simeq 12.4 \text{ m s}^{-1}$$

$$d\bar{U}_1/dx_2 \simeq 47 \text{ s}^{-1} \qquad L_{11,1} \simeq 51 \text{ mm}$$

$$u_1'/\bar{U}_c \simeq 5.0\% \qquad \lambda_{11} \simeq 5.8 \text{ mm}$$

$$u_2'/\bar{U}_c \simeq 3.0\% \qquad \eta \simeq 0.20 \text{ mm}$$

$$u_3'/\bar{U}_c \simeq 3.6\% \qquad R_{\lambda_1} \simeq 238$$

$$\overline{u_1u_2}/u_1'u_2' \simeq -0.45.$$

Here, the streamwise Taylor microscale is $\lambda_{11} = (\overline{u_1^2}/\overline{(\partial u_1/\partial x_1)^2})^{1/2}$, the Kolmogorov microscale is $\eta = (\nu^3/\varepsilon)^{1/4}$ and the turbulence Reynolds number is $R_{\lambda 1} = u_1'\lambda_{11}/\nu$.

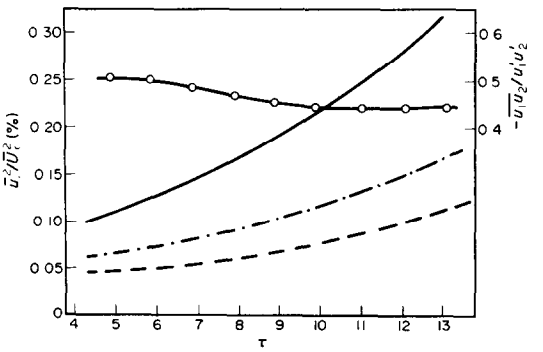

FIG. 2. Downstream development of Reynolds stresses. (——) $\overline{u_1^2}/\overline{U_c^2}$, (— — —) $\overline{u_2^2}/\overline{U_c^2}$, (—·—) $\overline{u_3^2}/\overline{U_c^2}$, (— ° —) $-\overline{u_1u_2}/u_1'u_2'$.

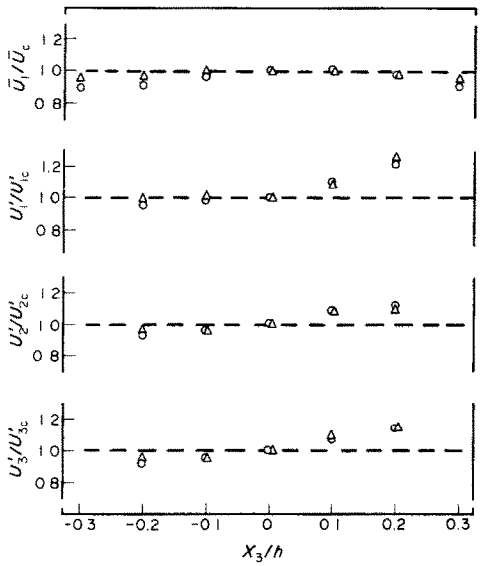

FIG. 3. Tests of spanwise homogeneity of the mean velocity and the r.m.s. turbulent velocities. (△) $\tau = 8.6$, (○) = 11; $x_2/h = 0.50$.

Measurement of D_{i2} *components*

In [13], the flow was heated electrically by cylindrical rods located along the midlines of the slot exits. The rods were identical and uniform, the voltage across each rod being individually adjusted, so that a mean temperature field with $\partial\bar{T}/\partial x_2 \simeq$ constant $\neq 0$ and $\partial\bar{T}/\partial x_3 \simeq 0$ was produced. It turned out that, away from the walls, $\partial\bar{T}/\partial x_1 \simeq 0$ also, so that the mean temperature gradient was parallel to the mean shear direction. The temperature rise $\Delta\bar{T}$ was small enough as to have no appreciable effect on the velocity field. Like the velocity fluctuations (although at a slower rate), the temperature fluctuations seemed to be approaching an asymptotic state, with mean squared values (Fig. 4) and their integral length scales monotonically increasing downstream. The two non-zero heat flux correlation coefficients, $\overline{\theta u_1}/\theta' u_1'$ and $\overline{\theta u_2}/\theta' u_2'$, were increasing very slightly at the downstream end of the test section (Fig. 4). The third component of the heat flux vector, zero by symmetry if the fields were perfectly generated, had a negligible normalized value $\overline{\theta u_3}/\theta' u_3'$. The transverse homogeneity of the temperature fluctuations and scales was comparable to that of the velocity fluctuations. The relevant experimental values at $\tau = 11.0$ were as follows ($\Delta\bar{T}_c$ is the centerline mean temperature rise)

$$\Delta\bar{T}_c \simeq 1.5°\text{C}$$

$$d\bar{T}/dx_2 \simeq 9.5°\text{C m}^{-1} \qquad |\overline{\theta u_3}/\theta' u_3'| < 0.02$$

$$\theta'/\Delta\bar{T}_c \simeq 7.7\% \qquad D_{12} \simeq -0.0042 \text{ m}^2 \text{ s}^{-1}$$

$$\overline{\theta u_1}/\theta' u_1' \simeq 0.56 \qquad D_{22} \simeq 0.0020 \text{ m}^2 \text{ s}^{-1}$$

$$\overline{\theta u_2}/\theta' u_2' \simeq -0.44 \qquad |D_{32}| < 0.0001 \text{ m}^2 \text{ s}^{-1}.$$

Measurements of D_{i3} *components*

A new experiment was designed specifically to provide values of the D_{i3} ($i = 1, 2, 3$) components. The commercial heating rods used in the earlier experiments were replaced by glass rods, 4 mm in diameter. The rods were wound with Nichrome heating wire (0.25 mm diameter, 20 Ω m^{-1}, respectively) after being covered with a thin layer of cement (Sauereisen No. 33) to prevent slip. The winding was made non-uniform with wire loop-spacing gradually increasing along each rod in a predesigned pattern which, after trial and error adjustments in the voltages and the windings, yielded a rough approximation to a uniform temperature gradient in the x_3 direction.

DISA hot-wires and cold-wires were used as velocity and temperature fluctuation sensors, while the mean temperature rise was measured with a pair of glass-coated thermistor probes.

x_2-Profiles of the mean temperature in the x_3 direction at three downstream stations are shown in Fig. 5. The profiles in the first two stations ($\tau = 4.3$ and

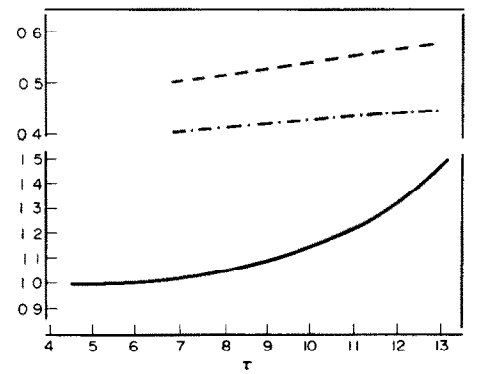

FIG. 4. Downstream development of temperature fluctuations and heat flux correlations for the case with $d\bar{T}/dx_2 \neq 0$. (——) $\overline{\theta^2}/\theta_\tau^2$ ($\theta_\tau^2 = 0.0137°\text{C}^2$), (— — —) $\overline{\theta u_1}/\theta' u_1'$, (— · — · —) $-\overline{\theta u_2}/\theta' u_2'$ [13].

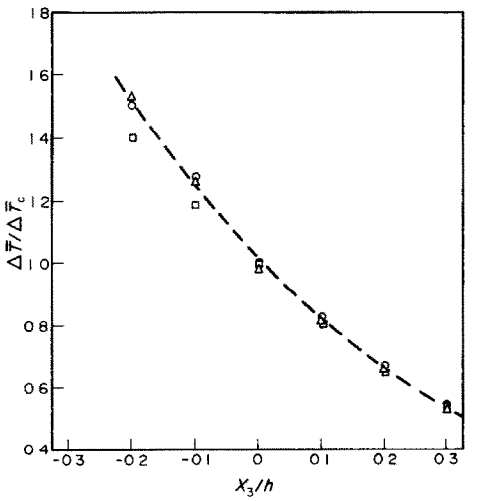

FIG. 5. Mean temperature rise for the case with $d\bar{T}/dx_3 \neq 0$. (○) $\tau = 4.4$, (△) $\tau = 8.6$, (□) $\tau = 12.6$; $x_2/h = 0.50$, (— — —) cubic polynomial fitted to the first two sets of data.

8.5) nearly coincide in the central half of the tunnel while the profile near the end of the test section ($\tau = 12.5$) deviates from the other two, indicating appreciable effects of boundary layer growth and of heat losses through the walls. Although the heating elements were designed to produce a constant $\partial\bar{T}/\partial x_3$, it turned out that $\partial\bar{T}/\partial x_3$ was monotonically decreasing in the direction of positive x_3. This variation can be attributed primarily to the crude nature of the preliminary calculations and, to a smaller degree, to non-uniformities of the velocity field. The change in $\partial\bar{T}/\partial x_3$ (Fig. 6), was about 25% for x_3 distances equal to an integral length scale. As a result, the r.m.s. temperature fluctuations θ' also varied in the x_3 direction by about an equal percentage. However, as shown in Fig. 6, quantities such as the ratio $\theta'/(\partial\bar{T}/\partial x_3)$, the heat transport correlation coefficient $\overline{\theta u_3}/\theta' u_3'$, and the diffusivity component D_{33}, showed much slower variation in the tunnel core. Consequently, the non-homogeneities of the temperature field were considered sufficiently weak for the present application; further improvement would have required considerably more time.

The purpose of the experiment was to produce a mean temperature field with a gradient in the x_3 direction only. As shown in Fig. 7, the mean temperature showed measurable variations also in the x_1 and x_2 directions, but the magnitudes of these undesirable gradients were relatively small compared to $\partial\bar{T}/\partial x_3$ in the central core of the tunnel at the main measuring station ($\tau = 11$). The estimated $\partial T/\partial x_2$ was less than 20% of the local $\partial\bar{T}/\partial x_3$ anywhere in the test volume, and considerably smaller in a restricted region about the axis. As a result, nonuniformities in the r.m.s. temperature fluctuations, θ', and the dominant heat flux correlation coefficient, $\overline{\theta u_3}/\theta' u_3'$, along the x axis were also relatively small (Fig. 8). Streamwise mean temperature gradients increased systematically near the end of the test section ($\tau = 12.5$), especially in the upper half of the flow, where heat losses through the walls are larger. Luckily, on the axis of the tunnel (Fig. 9), the mean temperature was practically constant.

Following the procedures outlined in [13] and assuming statistical stationarity and transverse homogeneity of both the velocity and the temperature

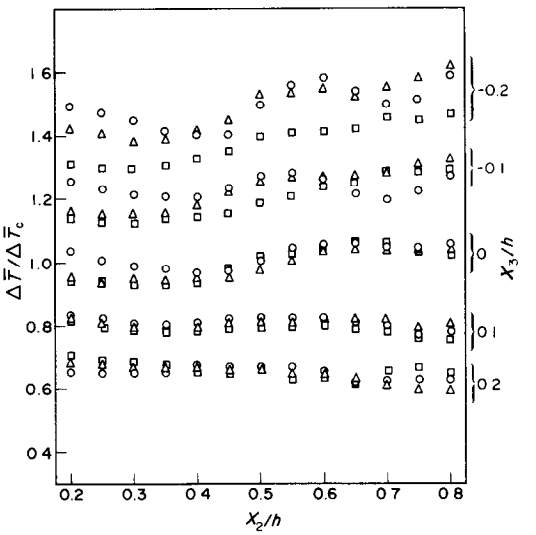

FIG. 7. Variation of the mean temperature rise in the central core of the measuring volume. (○) $\tau = 4.4$, (△) $\tau = 8.6$, (□) $\tau = 12.6$.

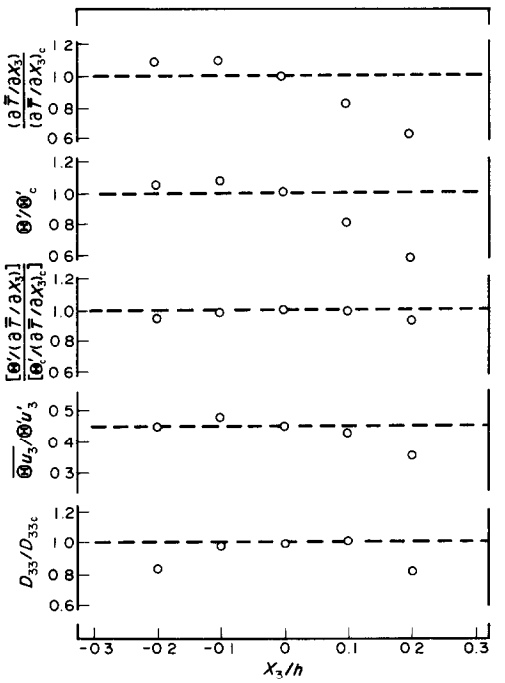

FIG. 6. Test of spanwise homogeneity of the temperature fluctuation field. $x_2/h = 0.50$, $\tau = 11$.

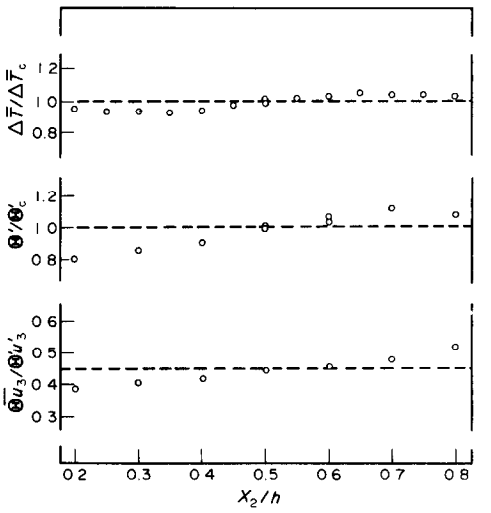

FIG. 8. Tests of transverse homogeneity of the temperature field, $x_3/h = 0.00$, $\tau = 11$.

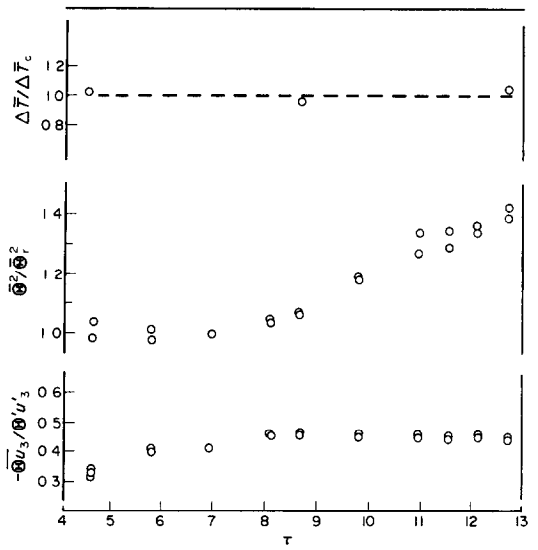

FIG. 9. Downstream evolution of the temperature field along the axis centerline. $x_2/h = 0.50$, $x_3/h = 0.00$.

fluctuation fields, the balance equations for the mean temperature and for the mean squared temperature fluctuations can be simplified as follows:

$$\frac{\partial}{\partial x_1}\left(\bar{U}_1\bar{T}+\overline{\theta u_1}-\gamma\frac{\partial\bar{T}}{\partial x_1}\right)\simeq 0 \tag{2}$$

and

$$\bar{U}_1\frac{\partial\overline{\theta^2}}{\partial x_1}\simeq -2\overline{\theta u_3}\frac{\partial\bar{T}}{\partial x_3}-2\gamma\overline{\frac{\partial\theta}{\partial x_i}\frac{\partial\theta}{\partial x_i}}. \tag{3}$$

Equation (2) is approximately satisfied since $\overline{\theta u_1}$ is experimentally found negligible while, experimentally also, $\partial\bar{T}/\partial x_1 \simeq 0$. Equation (3) states that the net growth rate of temperature fluctuations is equal to the difference between production rate by the mean gradient, and molecular destruction rate. No data on the latter are available; however, Fig. 9 shows that, for $\tau > 5$, there is a continuous downstream increase of the mean squared temperature fluctuations, indicating that production dominates over molecular destruction. The rate of increase of $\overline{\theta^2}$ in the present case is somewhat larger than that in the case with a mean temperature gradient parallel to the mean shear; some of this may be contributions from the unwanted mean gradient components in the x_1 and x_2 directions. As in the previous experiments, however, the field appears to approach an asymptotic development state, as indicated by the near constancy of the heat flux correlation coefficient for $\tau > 7$ (Fig. 9).

Measured values at $\tau = 11$, on the tunnel centerline are summarized below:

$\Delta\bar{T}_c \simeq 1.2°\text{C}$ $\quad |\overline{\theta u_1}/\theta' u_1'| < 0.05$

$|D_{13}| < 0.0005\ \text{m}^2\ \text{s}^{-1}$

$\partial\bar{T}/\partial x_3 \simeq 8.2°\text{C m}^{-1}$ $\quad |\overline{\theta u_2}/\theta' u_2'| < 0.06$

$|D_{23}| < 0.004\ \text{m}^2\ \text{s}^{-1}$

$\theta'/\Delta\bar{T}_c \simeq 11\%$ $\quad \overline{\theta u_3}/\theta' u_3' \simeq -0.45$

$D_{33} \simeq 0.0032\ \text{m}^2\ \text{s}^{-1}$.

Notice that $\overline{\theta u_3}/\theta' u_3'$ in the present experiment has about the same value as $\overline{\theta u_2}/\theta' u_2'$ in the case with dominant $\partial\bar{T}/\partial x_2$. As anticipated, the dominant component of D_{ij} is now D_{33}. The small, non-zero values of D_{13} and D_{23} can be attributed to inhomogeneities in the flow and possibly to inaccuracies in the alignment of the measuring probes.

In conclusion, the direct measurements of D_{ij} components were

$$[D_{ij}] \simeq \begin{bmatrix} \cdots & -2.2 & 0 \\ \cdots & 1.0 & 0 \\ \cdots & 0 & 1.6 \end{bmatrix} D_{22} \tag{4}$$

where D_{22} is factored out in order to emphasize ratios. Although it seems difficult to account for all possible sources of error, a likely estimate of the maximum uncertainty in equation (4) would be $\pm 10\%\ D_{22}$.

3. A THEORETICAL ESTIMATE USING MOSTLY MATERIAL COORDINATES

Consider a statistically homogeneous and stationary turbulent shear flow with a mean velocity vector given by

$$\bar{U}_i = \frac{\mathrm{d}\bar{U}_1}{\mathrm{d}x_2}x_2\delta_{i1}; \quad \frac{\mathrm{d}\bar{U}_1}{\mathrm{d}x_2} = \text{const.} \tag{5}$$

(overbars denote ensemble averages and δ_{ij} is Kronecker's delta). A quasi-Lagrangian velocity fluctuation, v_i^* [16, 17], can be defined by

$$v_i^*(\mathbf{X}_0, t) \equiv V_i(\mathbf{X}_0, t) - \frac{\mathrm{d}\bar{U}_1}{\mathrm{d}x_2}[X_2(X_0, t) - X_{02}]\delta_{i1} \tag{6}$$

where $\mathbf{X}_0$ is the initial position vector of a fluid particle (for convenience taken to be the origin of the coordinate system, so that $\mathbf{X}_0 = \mathbf{0}$) and V_i is the Lagrangian velocity of the particle. Apparently, v_1^* is not the traditional Lagrangian velocity fluctuation v_1, however, $v_2^* = v_2$ and $v_3^* = v_3$.

Next, consider a statistically homogeneous and stationary temperature field, passively superimposed on the velocity field. The initial temperature rise $\Delta T(\mathbf{X}_0, 0)$ is assumed to be a linear function of position [25]

$$\Delta T(\mathbf{X}_0, 0) = \frac{\partial\bar{T}}{\partial x_i}X_{0i} \tag{7}$$

and the mean temperature gradients $\partial\bar{T}/\partial x_i$ are assumed constant at all times. The latter assumption

can only be approximately satisfied, since shear tends to rotate transverse isotherms and, therefore, distort streamwise mean temperature gradients. Then, the instantaneous temperature fluctuation in material coordinates will be (neglecting molecular conduction)

$$\begin{aligned}\vartheta(X_0,t) &= \Delta T(X_0,0)-\Delta\bar{T}(X_0,t)\\ &= \frac{\partial\bar{T}}{\partial x_i}[X_{0i}-X_i]\\ &= -\frac{\partial\bar{T}}{\partial x_i}\int_0^t V_i(X_0,\tau)\,\mathrm{d}\tau. \end{aligned} \tag{8}$$

The heat flux vector (in homogeneous fields, one-point averages are the same in spatial and material coordinates, as shown by Lumley [26]), will be

$$\begin{aligned}-\overline{\theta u_i} &= -\overline{\vartheta v_i} = \frac{\partial\bar{T}}{\partial x_j}\int_0^t \overline{V_j(\tau)v_i(t)}\,\mathrm{d}\tau\\ &= \frac{\partial\bar{T}}{\partial x_j}\Bigg[\int_0^t \overline{v_j^*(\tau)v_i(t)}\,\mathrm{d}\tau\\ &\quad +\delta_{j1}\frac{\mathrm{d}\bar{U}_1}{\mathrm{d}x_2}\int_0^t\int_0^t \overline{v_2(\tau')v_i(t)}\,\mathrm{d}\tau'\,\mathrm{d}\tau\Bigg] \end{aligned} \tag{9}$$

with the initial positions X_0 omitted in the arguments.

Using a simplified expression of the double integral [27], equation (9) becomes

$$\begin{aligned}-\overline{\theta u_i} &\simeq \frac{\partial\bar{T}}{\partial x_j}\Bigg[\int_0^t \overline{v_i(0)v_j^*(\tau)}\,\mathrm{d}\tau\\ &\quad +\delta_{j1}\frac{\mathrm{d}\bar{U}_1}{\mathrm{d}x_2}\int_0^t \tau\,\overline{v_i(0)v_2(\tau)}\,\mathrm{d}\tau\Bigg]. \end{aligned} \tag{10}$$

For large diffusion times ($t\to\infty$), it is possible to define Lagrangian integral time scales, T_{ij}, and Lagrangian correlation moments, M_{ij}, as follows

$$T_{ij} = \frac{1}{\overline{v_i v_j}}\int_0^\infty \overline{v_i(0)v_j(\tau)}\,\mathrm{d}\tau \tag{11}$$

(i,j not summed)

and

$$M_{ij} \equiv \frac{1}{\overline{v_i v_j}}\int_0^\infty \tau\,\overline{v_i(0)v_j(\tau)}\,\mathrm{d}\tau \tag{12}$$

(i,j not summed).

Similarly, quasi-Lagrangian integral time scales, T_{i1}^*, can be defined as

$$T_{i1}^* \equiv \frac{1}{\overline{v_i v_1^*}}\int_0^\infty \overline{v_i(0)v_1^*(\tau)}\,\mathrm{d}\tau. \tag{13}$$

Then, the turbulent diffusivity tensor can be expressed in the following asymptotic form

$$[D_{ij}] \simeq \begin{bmatrix} \overline{v_1v_1^*}\,T_{11}^* + \overline{v_1v_2}\,M_{12}\dfrac{\mathrm{d}\bar{U}_1}{\mathrm{d}x_2} & \overline{v_1v_2}\,T_{12} & 0\\ \overline{v_2v_1^*}\,T_{21}^* + \overline{v_2^2}\,M_{22}\dfrac{\mathrm{d}\bar{U}_1}{\mathrm{d}x_2} & \overline{v_2^2}\,T_{22} & 0\\ 0 & 0 & \overline{v_3^2}\,T_{33}\end{bmatrix}. \tag{14}$$

Notice that, since x_3 is a direction of symmetry, $D_{13} = D_{31} = D_{23} = D_{32} = 0$. Expression (14) is obviously non-diagonal and non-symmetric since, in general, $D_{12}\neq D_{21}$.

Equation (14) is a theoretical result for the impossible case of homogeneous, stationary shear flow. Further, the Lagrangian and quasi-Lagrangian quantities in (14) are difficult to measure and they are not available for the present test case of nearly homogeneous shear flow. Therefore, it seems worthwhile to express (14) in terms of measurable quantities by involving connections, both exact and speculative, with Eulerian quantities. First [26], we replace Lagrangian by Eulerian one-point moments. Next, we speculate that the statistical properties of v_1^* are the same as those of v_1 (roughly checked in a numerical simulation of shear flow by Riley [22]), and thus can be approximated by Eulerian statistics. Similarly, we assume that T_{ij}, M_{ij} and T_{ij}^* can be approximated by their Eulerian counterparts in a frame travelling with the mean flow, i.e. that

$$T_{ij} \simeq T_{ij} = \int_0^\infty R_{ij}(\tau)\,\mathrm{d}\tau \tag{15}$$

$$M_{ij} \simeq M_{ij} = \int_0^\infty \tau\,R_{ij}(\tau)\,\mathrm{d}\tau \tag{16}$$

where

$$R_{ij}(\tau) \equiv \frac{\overline{u_i(0,0,0;0)\,u_j(\bar{U}_1\tau,0,0;\tau)}}{\overline{u_i u_j}} \tag{17}$$

(no summation).

Then, equation (11) can be approximated by

$$[D_{ij}] \simeq \begin{bmatrix} \overline{u_1^2}\,T_{11} + \overline{u_1u_2}\,M_{12}\dfrac{\mathrm{d}\bar{U}_1}{\mathrm{d}x_2} & \overline{u_1u_2}\,T_{12} & 0\\ \overline{u_1u_2}\,T_{21} + \overline{u_2^2}\,M_{22}\dfrac{\mathrm{d}\bar{U}_1}{\mathrm{d}x_2} & \overline{u_2^2}\,T_{22} & 0\\ 0 & 0 & \overline{u_3^2}\,T_{33}\end{bmatrix}. \tag{18}$$

For a qualitative comparison of the various D_{ij} components, expression (18) can be further simplified. Independent tests using the experimental values show that $R_{ij}(\tau)$ can be approximated by fitted exponential curves (except, in some cases, for the initial part) as

$$R_{ij}(\tau) \simeq \mathrm{e}^{-\tau/T_{ij}} \tag{19}$$

which implies that

$$M_{ij} \simeq \int_0^\infty \tau\, e^{-\tau/T_{ij}}\, d\tau = T_{ij}^2. \qquad (20)$$

Then, expression (18) can be approximated by

$$[D_{ij}] \simeq \begin{bmatrix} \overline{u_1^2}\, T_{11} + (\overline{u_1 u_2}\, T_{12}) \left(T_{12} \dfrac{d\bar{U}_1}{dx_2} \right) & \overline{u_1 u_2}\, T_{12} & 0 \\ \overline{u_1 u_2}\, T_{21} + (\overline{u_2^2}\, T_{22}) \left(T_{22} \dfrac{d\bar{U}_1}{dx_2} \right) & \overline{u_2^2}\, T_{22} & 0 \\ 0 & 0 & \overline{u_3^2}\, T_{33} \end{bmatrix} \qquad (21)$$

which contains directly measurable terms.

4. VARIOUS ESTIMATES OF DIFFUSIVITY COMPONENTS

A crude evaluation of the theoretical expressions

The accuracy of the theoretical expressions derived in the earlier section can be tested vs the direct measurements, equation (4). Since several quantities in the exact relation (14) have not been measured, we shall instead consider the approximate relation (18). The various scales and moments were estimated from measurements of $R_{11}(\tau)$, $R_{12}(\tau)$ and $R_{22}(\tau)$ [12]. Because only initial parts of these correlations were available, the data were extrapolated to infinity by fitted exponential functions (Fig. 10). As shown in Fig. 11, the extrapolated parts had significant extent, especially for the R_{12} curve. The first moments of R_{22} and R_{12}, shown in Fig. 12, had even more significant contributions from the extrapolated regions. Integration of the corresponding curves provided the following estimates

$$T_{11} \simeq 0.054 \text{ s} \qquad M_{12} \simeq 0.0099 \text{ s}^2$$

$$T_{12} \simeq 0.100 \text{ s} \qquad M_{22} \simeq 0.00078 \text{ s}^2$$

$$T_{22} \simeq 0.0027 \text{ s}.$$

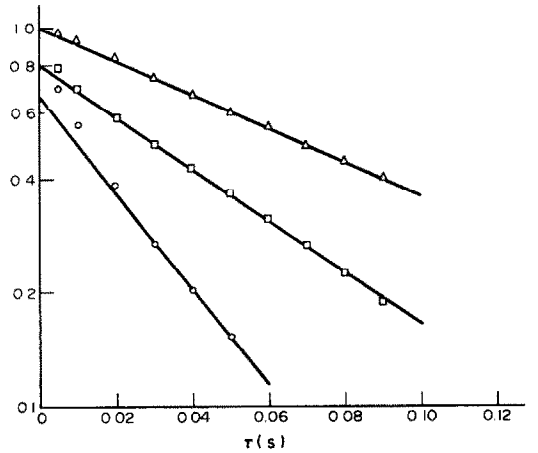

FIG. 10. Eulerian velocity correlation coefficients in a convected frame. Measurements [12]: (□) $R_{11}(\tau)$, (○) $R_{22}(\tau)$, (△) $R_{12}(\tau)/R_{12}(0)$, (——) fitted exponential functions excluding initial points.

In the absence of any relevant measurements of the remaining quantities in (18), we shall assume that

$$T_{21}^* \simeq T_{12} \quad \text{and} \quad T_{33} \simeq T_{22}.$$

Substituting these values in (18), we get

$$[D_{ij}] \simeq \begin{bmatrix} (5.7\text{–}13.0) & -2.9 & 0 \\ -2.9+1.3 & 1.0 & 0 \\ 0 & 0 & 1.5 \end{bmatrix} D_{22}. \qquad (22)$$

D_{11}/D_{22} is bracketed because the net negative value seems physically paradoxical and could result partially from the extensive extrapolation used in the M_{12} estimate. Another point of concern is that the average flight time of fluid particles in the wind-tunnel test section was about 0.25 s, not several orders of magnitude larger than T_{12}, as required for the above estimate of M_{12} to be meaningful. In any case, the second and third columns of (4) and (22) are in reasonable agreement. Also, D_{12}/D_{21} in (22) is not too far from its estimate by Gee and Davies [10]. The ratio D_{33}/D_{22} was about 1.5, corresponding to the ratio $\overline{u_3^2}/\overline{u_2^2}$. A $\pm 10\%$ D_{22} maximum error for the determination of the D_{ij} components from measurements appears plausible. However, it seemes impossible to evaluate the inaccuracies in expression (21), which could, presumably, result in substantial errors in (22).

Estimates based on a numerical simulation

The numerical simulation of homogeneous shear flow described by Riley [22] and summarized partially by Riley and Corrsin [21], contains sufficient information for estimating all components of D_{ij}. The method involved the mathematical modelling of a random Eulerian velocity field and the computation of its statistical properties over ensembles of independent realizations. The model differed from a Navier–Stokes flow since it contained no interactions among the different wave numbers.

Certain properties of the model were selected to match the statistics of the experimental flow studied by Champagne *et al.* [28]. For example, the principal axes of the Reynolds stress tensor, the ratios of turbulent kinetic energies and the ratios of integral length scales along the different axes were approximately the same in the two cases. Unlike the experiments of Harris *et al.* [12], and Tavoularis and Corrsin [13], the flow of

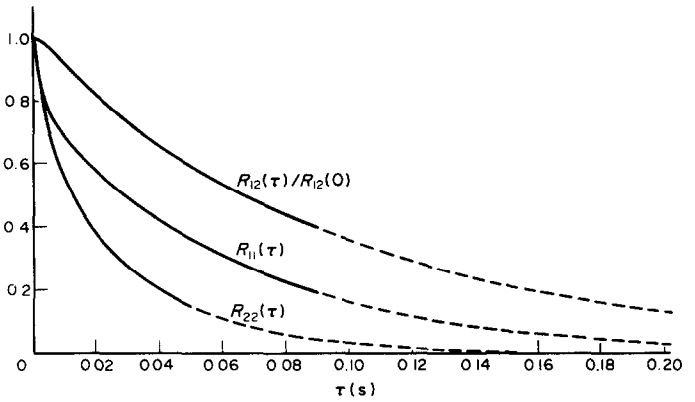

FIG. 11. Eulerian velocity correlation coefficients in a convected frame, (——) measured ranges, (---) extrapolated ranges.

Champagne *et al.* [28] had not reached a state of asymptotic development in the wind-tunnel test section, due to the insufficiently large total strain (about one-third of that in the other two experiments). Therefore, some differences in the diffusivity ratios between the high shear and the low shear experiments should be expected.

Ratios of the diffusivity components evaluated directly by Riley [22] are shown in Fig. 13. Although these ratios, especially $(D_{12}+D_{21})/D_{22}$, showed large fluctuations during the numerical experiment, their means were fairly constant, typically as follows:

$$[D_{ij}] \simeq \begin{bmatrix} 1.9 & — & 0 \\ — & 1.0 & 0 \\ 0 & 0 & 1.2 \end{bmatrix} D_{22} \qquad (23)$$

$$D_{12}+D_{21} \simeq -0.9\,D_{22}.$$

The separate values of non-diagonal terms were not computed. For comparison with (23), one can estimate the asymptotic theoretical terms of equation (14), using the appropriate Lagrangian and quasi-Lagrangian values determined from the simulation. The corresponding (prescribed or "measured") values in arbitrary units were

$$\begin{aligned} d\bar{U}_1/dx_2 &= 1 & T^*_{11} &= 0.61 & M^*_{12} &= 0.50 \\ \overline{v_1^{*2}} &= 1.86 & T_{22} &= 0.54 & M_{22} &= 0.29 \\ \overline{v_2^2} &= 0.89 & T_{33} &= 0.54 & & \\ \overline{v_3^2} &= 1.06 & T^*_{12} &= 0.63 & & \\ \overline{v_1^* v_2} &= -0.52 & T^*_{21} &= 0.81. & & \end{aligned}$$

Assuming that $\overline{v_1 v_1^*} \simeq \overline{v_1^{*2}}$, $\overline{v_1 v_2} \simeq \overline{v_1^* v_2}$, $T_{12} \simeq T^*_{21}$ and $M_{12} \simeq M^*_{12}$ and substituting the values into (14), one gets

$$[D_{ij}] \simeq \begin{bmatrix} (2.4-0.7) & -0.7 & 0 \\ (-0.9+0.5) & 1.0 & 0 \\ 0 & 0 & 1.2 \end{bmatrix} D_{22}. \qquad (24)$$

The diagonal terms and the sum $(D_{12}+D_{21})/D_{22}$ are roughly the same in (23) and in (24). The ratio $D_{21}/D_{12} \simeq 0.57$, close to the values 0.55 in (22) and 0.5 in Gee and Davies' [10] estimate.

Estimates based on a rapid distortion type analysis

Kozlov and Sabel'nikov [23] have studied the evolution of the turbulent diffusivity components of

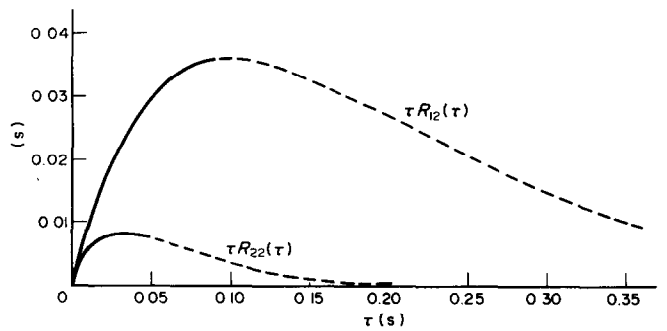

FIG. 12. Eulerian velocity correlation moments, (——) measured ranges, (---) extrapolated ranges.

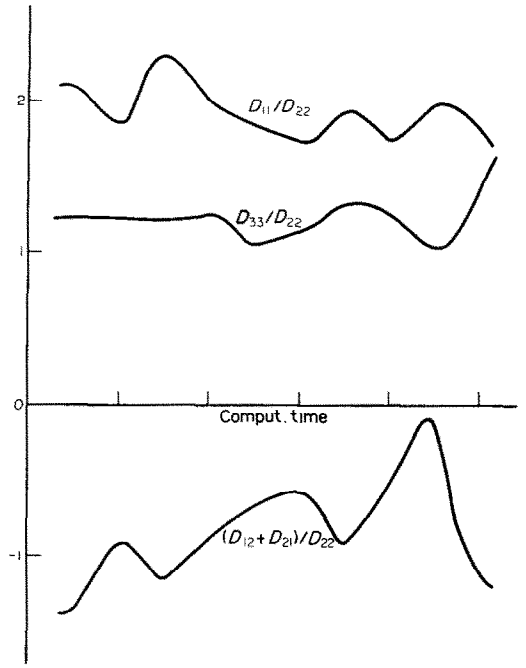

FIG. 13. Turbulent diffusivity ratios in a numerical simulation of homogeneous shear flow [22].

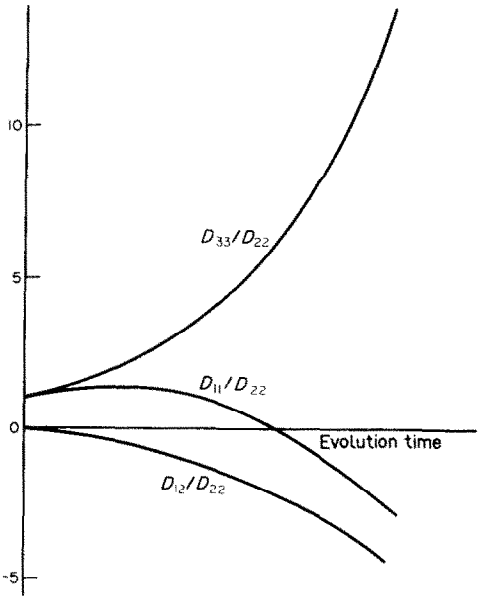

FIG. 14. Turbulent diffusivity ratios based on a rapid distortion type analysis [23].

initially isotropic turbulence subjected to uniform shear. The distortion is assumed to be sufficiently rapid for the non-linear (inertial) interactions of the velocity fluctuations to be negligible. Theoretical expressions for the diffusivities, similar to the ones presented in Section 3 (although it is now assumed that $D_{12} = D_{21}$), are first derived, then expressed in spectral forms and finally integrated numerically. The resulting diffusivity ratios are shown in Fig. 14. The ratios vary continuously with increasing total strain and do not demonstrate any asymptotic trends in the reported range. The value of D_{33}/D_{22} was totally unrealistic, exceeding 13 for the highest total strain. The behaviour of D_{11}/D_{22} is rather peculiar. First, it increases slightly from the isotropic value 1.0 to a maximum of about 1.4, then it decreases monotonically and becomes negative, with a value -2.5 corresponding to the highest total strain. These negative values of D_{11}/D_{22} provide qualitative support for the similar finding in equation (16). The ratios D_{12}/D_{22} and D_{21}/D_{22} decrease monotonically from the isotropic value 0.

5. DISCUSSION AND CONCLUSIONS

The components of the turbulent diffusivity tensor in homogeneous sheared turbulence have been estimated using several distinct experimental and analytical techniques. Considering the approximate nature of techniques used and the observed discrepancies in certain cases, it appears necessary to re-evaluate and compare the different results in detail.

Most reliable appear to be the direct measurements, equation (4), but unfortunately they do not contain the D_{i1} components. In any case, the existing measurements are in fair agreement with the corresponding theoretical estimates in equation (22). The numerical estimates of D_{ij}, equations (23) and (24), demonstrate qualitative similarities with (4) and (22) but the individual values are different. It should be remembered that the results in (23) and (24) correspond to a flow with much smaller mean shear than do these in (4) and (22). It is logical to expect that the low-shear diffusivity ratios should be closer to the isotropic values than are the high-shear ones, especially in view of the evidence that the low shear experiment ([28]; see discussion in [12]) had not reached its asymptotic structure.

Indeed, (23) and (24) show smaller deviations from the unit tensor than do (4) and (22). A reasonable speculation is that the diffusivity ratios, like the principal stress axes, depend on the total strain imposed on turbulence.

The most intriguing result of the present study has been that, contrary to the intuitive notion of diffusivity, D_{11} may be negative. This possibility can be explored with the use of the approximate theoretical estimate, equation (21).

For the homogeneous shear flow, $\overline{u_1 u_2} < 0$, while all scales T_{ij} can be assumed to have the same order of magnitude. Then

$$D_{11} \simeq \overline{u_1^2}\, T_{11}\left(1 - K_1 T_{11}\frac{\mathrm{d}\bar{U}_1}{\mathrm{d}x_2}\right) \tag{25}$$

where K_1 is a positive parameter of order unity

$$K_1 = \frac{-\overline{u_1 u_2}}{\overline{u_1^2}}\left(\frac{T_{12}}{T_{11}}\right)^2. \tag{26}$$

Since the relative magnitudes of turbulent stresses and of integral scales in different directions are only weak functions of mean shear, it seems plausible that, for large enough $d\bar{U}_1/dx_2$, the second term in (22) may exceed unity, thus resulting in negative D_{11}. This possibility was supported by the rapid distortion calculation, as shown in Fig. 13.

Another consequence of equation (21) is that the degree of asymmetry of D_{ij}, expressed as the ratio D_{21}/D_{12}, is also a function of mean shear

$$\frac{D_{21}}{D_{12}} \simeq 1 - K_2 T_{12} \frac{d\bar{U}_1}{dx_2} \tag{27}$$

where K_2 is also a positive parameter of order unity

$$K_2 = \frac{\overline{u_2^2}}{-\overline{u_1 u_2}} \left(\frac{T_{22}}{T_{12}}\right)^2 \tag{28}$$

and $T_{12} \simeq T_{21}$ for convenience. Although not observed in the present study, it even appears possible that, for large enough $d\bar{U}_1/dx_2$, D_{21} may become zero or positive, while D_{12} must remain negative. It is hoped that future experiments in homogeneous shear flow with streamwise mean temperature gradient will help resolve these questions.

The present estimates apply mainly to a hypothetical homogeneous turbulence with a uniform mean shear, a case with rather limited practical significance. However, the results should also be applicable to a wider class of turbulent flows, namely nearly parallel flows with small transverse inhomogeneities and slowly variable mean gradients. For example [13], the ratio D_{12}/D_{22} was roughly the same in the nearly homogeneous turbulent shear flow, in a turbulent boundary layer at one momentum thickness distance from the wall, and in a turbulent pipe flow at a half the radius distance from the axis.

Fortunately, lack of accurate estimates for the D_{i1}, $i = 1, 2, 3$ components seems to be no serious problem for many practical applications, where the dominant mean temperature gradient is perpendicular to the mean flow direction. In such cases, the overall heat transfer is determined mainly by the D_{i2} and D_{i3} components and even gross inaccuracies in the D_{i1} estimates might have small contributions to the total error.

Acknowledgement—This research program has been supported primarily by the U.S. National Science Foundation, Program on Atmospheric Sciences.

REFERENCES

1. S. Corrsin, Limitations of gradient transport models in random walks and in turbulence, *Adv. Geophys.* **184,** 25–60 (1974).
2. K. R. Sreenivasan, S. Tavoularis and S. Corrsin, A test of gradient transport and its generalizations, *Turbulent Shear Flows* **3,** 96–112 (1983).
3. B. E. Launder, Heat and mass transport, *Turbulence, Topics appl. Phys.* **12,** 231–287 (1976).
4. G. K. Batchelor, Diffusion in a field of homogeneous turbulence, *Austr. J. Sci. Res.* **A2,** 437–450 (1949).
5. K. L. Calder, On the equation of atmospheric diffusion, *Q. J. R. Meteor. Soc.* **91,** 514–517 (1965).
6. G. I. Taylor, Diffusion by continuous movements, *Proc. Lond. Math. Soc.* **20,** 196–213 (1921).
7. C. Eckart, An analysis of the stirring and mixing processes in incompressible fluids, *J. Mar. Res.* **7,** 265–275 (1948).
8. H. Lettau, On eddy diffusion in shear zones, *Geoph. Res. Pap.* **19,** 437–445 (1952).
9. H. Matsuoka, Note on two-dimensional diffusion in the atmospheric surface layer, *J. Met. Soc. Japan* **39,** 324–330 (1961).
10. J. H. Gee and D. R. Davies, A further note on horizontal dispersion from an instantaneous ground source, *Q. J. R. Met. Soc. Lond.* **90,** 478–480 (1964).
11. A. M. Yaglom, Horizontal turbulent transport of heat in the atmosphere and the form of the eddy diffusivity tensor, *Fluid Dyn. Trans.* **4,** 801–812 (1969).
12. V. G. Harris, J. A. Graham and S. Corrsin, Further experiments in nearly homogeneous turbulent shear flow, *J. Fluid Mech.* **81,** 657–687 (1977).
13. S. Tavoularis and S. Corrsin, Experiments in nearly homogeneous turbulent shear flow with a uniform temperature gradient, Part I, *J. Fluid Mech.* **104,** 311–347 (1981).
14. R. G. Deissler, Turbulent heat flux and temperature fluctuations in a field with uniform velocity and temperature gradients, *Int. J. Heat Mass Transfer* **6,** 257–270 (1963).
15. J. Fox, Turbulent temperature fluctuations and two-dimensional heat transfer in a uniform shear flow, *NASA Tech. Note* D-2511 (1964).
16. S. Corrsin, Remarks on turbulent heat transfer, *Proc. Iowa Thermodyn. Sympos.* 5–28 (1953).
17. S. Corrsin, Progress report on some turbulent diffusion research, *Adv. Geophys.* **6,** 161–164 (1959).
18. J. J. Riley and S. Corrsin, The relation of turbulent diffusivities to Lagrangian velocity statistics for the simplest shear flow, *J. Geophys. Res.* **79,** 1768–1771 (1974).
19. S. Corrsin, A theoretical estimate of the turbulent diffusivity tensor in homogeneous shear flow, (Abstract), *Bull. Am. phys. Soc.* **18,** 1473 (1973).
20. J. L. Lumley, Turbulent transport of passive contaminants and particles: fundamentals and advanced methods of numerical modeling, *Pollutant Dispersal Lecture Notes,* von Karman Institute for Fluid Dynamics, Rhode-St.-Genese, Belgium, May (1978).
21. J. J. Riley and S. Corrsin, Simulation and computation of dispersion in turbulent shear flow, *Proc. Conf. Air Pollut. Met., Am. Met. Soc.* 16–21 (1971).
22. J. J. Riley, Computer simulations of turbulent dispersion, Ph.D. Dissertation, The Johns Hopkins University, Baltimore (1971).
23. V. E. Kozlov and V. E. Sabel'nikov, Turbulent diffusion in fast homogeneous shear of turbulence, *Fluid Dyn.* **12,** 940–942 (1977).
24. C. K. G. Lam and K. Bremhorst, Prediction of turbulent heat fluxes and temperature fluctuations, *Lett. Heat Mass Transfer* **6,** 489–501 (1979).
25. S. Corrsin, Heat transfer in isotropic turbulence, *J. appl. Phys.* **23,** 113–118 (1952).
26. J. L. Lumley, Some problems connected with the motion of small particles in turbulent fluid, Ph.D. Dissertation, The Johns Hopkins University, Baltimore (1957).
27. J. Kampé de Feriet, Les fonctions aléatoires stationnaires et la théorie statistique de la turbulence homogène, *Ann. Soc. Sci. Brux.* **59,** 145–194 (1939).
28. F. H. Champagne, V. G. Harris and S. Corrsin, Experiments on nearly homogeneous turbulent shear flow, *J. Fluid Mech.* **41,** 81–139 (1970).

EFFET DU CISAILLEMENT SUR LE TENSEUR DE DIFFUSIVITE TURBULENTE

Résumé—Des mesures antérieures de quelques composantes du tenseur de diffusivité turbulente D_{ij} dans un écoulement turbulent de cisaillement presque homogène, avec un gradient de température moyenne parallèle au cisaillement moyen sont complétées ici par des mesures de composantes additionnelles dans le même écoulement mais avec un gradient de température perpendiculaire à la fois à la vitesse moyenne et au cisaillement moyen. Une analyse quasi-lagrangienne fournit des expressions pour toutes les composantes de D_{ij} et confirme que D_{ij} est ni diagonal, ni symétrique. L'analyse suggère aussi la possibilite que D_{11} et D_{12} deviennent positifs à des valeurs suffisamment grandes du cisaillement moyen. On rapporte aussi des estimations de D_{ij} basées sur la simulation numérique de l'écoulement de cisaillement homogene et sur une analyse de distorsion rapide.

EINFLUSS EINER SCHERUNG AUF DEN TURBULENTEN DIFFUSIONSTENSOR

Zusammenfassung—Die früheren Messungen einiger Komponenten des turbulenten Diffusionstensors D_{ij} in einer nahezu homogenen turbulenten Scherströmung mit einem konstanten Gradienten der mittleren Temperatur, welcher parallel zur Haupt-Scher-Richtung ist, werden nun ergänzt durch die Messungen zusätzlicher Komponenten in derselben Strömung, aber mit einem Gradienten der mittleren Temperatur, der senkrecht zur Hauptströmungs- und Hauptscherungs-Richtung ist. Eine Quasi-Lagrange-Analyse liefert für alle Komponenten von D_{ij} Ausdrücke und bestätigt die Erwartung, daß D_{ij} weder diagonal noch symmetrisch ist. Die Analyse läßt auf die Möglichkeit schließen, daß D_{11} und D_{21} bei gegügend großen Werten der Hauptscherung positiv werden könnten. Unabhängige Abschätzungen von D_{ij}, welche sowohl auf der numerischen Simulation einer homogenen Scherströmung basieren, als auch auf einer schnellen Störungsanalyse, werden ebenfalls aufgeführt.

ВЛИЯНИЕ СДВИГА НА ТЕНЗОР ТУРБУЛЕНТНОЙ ДИФФУЗИИ

Аннотация—В дополнение к ранее выполненным измерениям ряда компонентов тензора турбулентной диффузии D_{ij} в почти однородном турбулентном сдвиговом потоке с постоянным значением среднего градиента температуры, направленного параллельно среднему касательному напряжению, в данной работе проведены измерения еще ряда компонентов для того же течения, где, однако, средний градиент температуры направлен перпендикулярно как к средней скорости, так и среднему касательному напряжению. В результате проведенного анализа, близкого к лагранжевому, получены выражения для всех компонентов D_{ij} и подтверждено предположение о том, что тензор D_{ij} является недиагональным и несимметричным. Показано, также, что при достаточно больших значениях среднего касательного напряжения D_{11} и D_{21} могут быть положительными. Даны оценки тензора D_{ij} на основе численного моделирования однородного сдвигового течения, а также анализа методом внезапного внесения возмущения.